Computer Science Journal of Moldova, vol.**28**, no.2(83), 2020

Hospital-Scale Chest X-Ray Database Visualization Using RAWGraph Technique

Haneen Hassan Al-Ahmadi

Abstract

For identification and screening of several lung diseases, the chest X-ray is just one of the very most often obtainable radiological tests. Most modern-day hospitals' Photo Archiving and Communication Systems (PACS) collect thousands of X-ray imaging scientific studies, followed by radiological stories that are collected and saved. In this paper, we employ the graph strategy to collect and store the dataset of those X-ray pictures. The RAWGraph can be an open source web tool for its production of inactive information visualizations, which can be changed to become further altered. Initially designed for picture artists to extend a succession of responsibilities, maybe not available in combination with different applications, it has developed into a stage that offers easy tactics to map information measurements on visual factors. That poses a more chart-based way of information visualization; every visual version will be an unaffiliated module displaying distinct visual factors that may be utilized to map information measurements. Thus, end-users may develop complex information visualizations. We assess the correlation and relationship among different aspects of this data set. We now provide a chest X-ray database, particularly "ChestX-ray8", that contains 108,948 frontal perspective X-rays of 32,717 specific and distinct patients, with all containing a written text created from eight disorder image tags (where just about every image could have multi-labels), in the related reports utilizing standard language processing. In this paper, we use diverse methods for visualization, which can be Circle Packing, Bee Swarm Plot, Convex Hull, Boxplot, and Circular Dendrogram. We image the

dataset more accurately and examine the terms of these various arrangements of features precisely.

Keywords: data visualization, x-rays, graphs, visualization tools, visual interface

1 Introduction

Using information visualization is standard procedure in most medical areas. Even though most visual variations are understood and have been used from the last several decades, their production remains difficult without human end users involvement. Although the current evolution of visualization libraries has empowered the production of innovative and very personalized options, continual programming comprehension and also a great deal of time are necessary to perfect the equipment [1]. The theory that guides RAW forging would be essential to supply an infrastructure to automatically create graphs where only minimal programming abilities are necessary, and the graphs can be reused together with their data. Beginning with the knowledge from design laboratory, then further researching together through papers, we understood that the production visualization procedure is not linear. Ergo, it cannot be solved utilizing one software [1]. Therefore, when planning visualizations, it is reasonable to proceed from device to software based on the use and process, however, we need to get a specific outcome. So, we then created a stage to accomplish this difficult endeavor with no code for the design of information measurements on rare visual variations. The results from this stage must be understood as easily available and alterable; this also usually means they are specifically built to become additionally altered and enhanced with secondary applications, such as vector images editors, including Adobe Illustrator, Inkscape and vectr.com [2].

Initially imagined as something for both designers and vis geeks, raw data is utilized to make a connection involving commonly available software such as Microsoft Excel, the Apple library Open Refine, along with vector image editors such as Adobe Illustrator and Inkscape. This is predicated around the SVG format [3], where visualizations are

readily erased and edited, and then used by vector images software for additional refinements or embedded into website pages. We recognize the importance of dealing with and protecting using sensitive information. The information is routed raw from and is processed solely from the Internet browser without any matter data storage or operation that has been completed. In this case, we will probably amend, copy, or otherwise alter our data. RAW can also be exceptionally customizable and flexible, enabling new, custom-made graphs characterized by end-users. To learn more regarding ways to edit or add graphs, visit the developer manual [4].

2 Literature Review

There have been efforts to generate publicly accessible, post-secondary health image databases using number of individuals who have been tested amount that ranges from a few hundred to two million records. However, no qualitative disorder detection answers have been already reported [5]. Our freshly suggested chest X-ray database, in term of size order, will be a minimally larger than OpenI. To attain the improved clinical significance, we now concentrate on exploiting the organizational operation of weakly-supervised, multi-label picture classification and disorder localization of frequent sinus ailments; into this standard measure the "discovering characteristics" or "visible modeling" are also included. Chest X-rays [6], entire lung tomograms, and surgical findings are associated with 152 patients having an extra thoracic malignancy who experienced 182 thoracotomies for their test of pulmonary nodules. Several pulmonary nodules are revealed through complete lung tomography, including one of 25 patients using a typical chest X-ray. Only two of 25 patients experienced carcinoma together with bilateral nodules, illustrated by tomography. Of all 64 patients having unilateral nodules found by traditional chest X-ray," 10 of 32 exhibited sarcoma, and two more with melanoma [7]. To make the conclusion in the scope of sinus metastasis in patients, lung tomograms or something similar with tomographic examinations [8] are the most efficient method of observation.

A sizable level screen with moderate amount of resolution with TV-fluoroscopic technique is using a 43 cm × 43 cm center, which has been utilized to track patients undergoing radiation treatment with mega-voltage remedy beams. The following report reveals some preliminary outcomes made for 60Co and 6 MV x-rays. The brain, the supraclavicular region, both the chest, along with lymph areas, are imaged. The stay video graphics show lung and heart, along with diaphragm movement. Except for the gut, different filing arrangements have been also displayed. Permanent files are manufactured on videotape or video disc drive. Moreover, the corresponding confirmation films have been displayed in every case [9]. Increased picture quality can readily be accessed with hardware. The movie graphics can easily be enriched by exclusive optical circuitry that's available at an affordable price. In this paper, we provide a way to extract bronchus spots from 3D CT pictures of lung shots from a helical CT scanner and then to describe them as 3D-shaded pictures. The extraction treatment comprises a 3D region expanding with all the parameters corrected mechanically and will be achieved immediately using a 3D painting algorithm. The result can be envisioned by PC images workstations, and also, the bronchus is seen out of the interior the same as using the simulated bronchus endoscope, openly and with no pain. We predict that manner of updating "navigation" [10].

From the current analysis, the feasibility of employing high-performance microtomography (Micro CT) for discovery of lung cancer has been researched in mice that were living in a heightened phase of cyst progress. The chest field of anesthetized mice had been reimaged by X-ray Micro CT [11]. In mice having a slight and significant chemical loading, Micro CT was always a quick and noninvasive imaging apparatus for the discovery of lung cysts. After the identification of their CT statistics by histologic sectioning, it had been shown that the majority of microbes could be differentiated from the rebuilt digital bits received by Micro CT. The info from Micro CT was additionally proved when supported by a visible review of their excised lungs post-mortem. Micro CT opens great perspectives for imaging enzyme development, and also its particular development as a noninvasive method [12]. The

Micro CT also enables for a routine test of lung cancer from medication. Many X-ray CT scanners demand only a couple seconds to create one two-dimensional (2D) picture of the cross-section of a human body. The truth of full-scale three-dimensional (3D) graphics of this human body synthesized by an adjacent collection of 2D pictures developed by successive CT scans of adjoining human anatomy pieces are tied to number of functions, such as: *i*) slice-to-slice enrollment (placement of the affected individual); *ii*) slit thickness; and also *iii*) movement, both voluntary and involuntary (which happens through the entire time necessary to scan all of pieces. For that reason, this way is insufficient for legitimate energetic 3D imaging of organs, including the lungs, heart, and flow. For resolving these issues, the Dynamic Spatial Reconstructor (DSR) was created from the Biodynamics Research Unit in the Mayo Clinic to present uninterrupted volumes of imaging. These are stop action (1/100 therefore), high-repetition-rate (up-to 60/s), a simultaneous scan of several concurrent sparse cross segments (up to 240, just about every 0.45-millimeter-thick, thick 0.9 mm aside) crossing the whole anatomic degree of the physiological organ(s) of attention [13]. These capacities are accomplished using multiple X-ray resources and several 2D fluoroscopic video-camera assemblies onto a continually rotating gantry. The desired trade-offs between temporal, spatial, and frequency settlement might be performed by retrospective processing and selection of typical subsets of their overall data listed via an ongoing DSR scanning arrangement.

3 Construction of Hospital-scale Chest X-ray Database

In this paper, we clarify the approach of constructing a hospital-scale chest X-ray image database, particularly "ChestX-ray8", created in our magician's PACS technique. To begin with, we shortlisted eight shared nasal pathology keywords, which are many times identified and observed on numerous occasions, i.e., Atelectasis, Cardiomegaly, Effusion, Infiltration, Mass, Nodule, Pneumonia, along with Pneumotho-

rax, dependent on radiologists' suggestions. Considering these eight keywords, we hunt the PACS strategy to extract all of the linked radiological stories (along with graphics) as our database corpus [14]. Several pure Natural Language Processing (NLP) methods have been accommodated for discovering the pathology like stop word removal, frequent word removal, rare word removal [15]. Every single record will probably undoubtedly be linked to a couple of keywords or marked using "Normal" in the desktop classification. As a consequence of that search, the ChestX-ray8 database consists of all 108,948 frontal-view X-ray pictures (resulting from 32,717 patients), and just about every picture is tagged with multiple or one pathology keywords.

3.1 Stop words removal

We have discussed stop words removal earlier in basic feature extraction from database. In basic pre-processing we have followed the same earlier routine. We have used a predefined library and also used a list of stop words.

3.2 Frequent words removal

In the previous step, we have just removed stop words, but in this step, we have removed common words. We have collected the ten most frequently occurring words, then take a call to retain or remove. We have removed those words that are not used in classification of the database.

3.3 Rare words removal

In the prior step we have removed the most common words, and in the next step we have removed the most rare words from the database. Due to the rarity, the association between them and other words is dominated by noise. We can replace the rare words with the general word form to increase the count of the words.

3.4 Labeling Disease Names by Text Mining

In general, our strategy generates tags by employing the accounts from two moves. From the very first iteration, we discover most of the disorder theory from the corpus. The most crucial figure of just about every chest X-ray report is commonly ordered as "Replies", "Indication", "Findings", and "Perception" segments. We give attention to discovering illness theories from the Indication and Perception segments. When an account comprises neither of the two segments, the full report is then going to be viewed. At the second pass, we follow the accounts. As a rule, they should not consist of any disorders (maybe not confined by two adjoining pathologies).

4 RawGraph Visualization Results

In this section, we focuse on different sets of visualization. It presents a chart-based approach to data visualization; each visual model is an independent module exposing different visual variables that can be used to map data dimensions. Consequently, users can create complex data visualizations. We have the lung disease dataset, which has 5607 rows of the dataset. In each row we have any specific data on males and females. In the first set of visualization, we upload the first 500 rows of diseases in RAWGraphs that are as shown in Figure 1.

4.1 RAWGraph Interface

In the interface of the RAWGraph, we can map the dimension of our interest in work more appropriately. After uploading the dataset, we can set our dimensions in different perspectives. We can set the hierarchy where we can drag number strings and dates, strings that we can drag here could use the gender and age of the patient. In section Hierarchy we can set the hierarchy of our data so, that the records to be ordered by patient's gender or age; in this section we can drag numbers, strings or dates for the data; string data are used for Patient Gender and numbers are used for Patient Age. In section Size we can set the age, where we can drag just the numbers for the age of the patient. In section Color we can set the Patient ID by dragging the

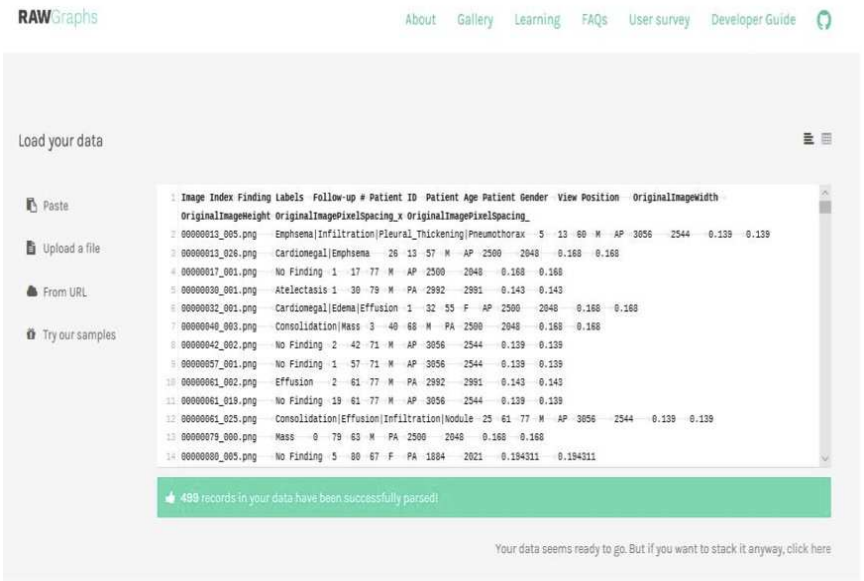

Figure 1. 500 rows of lungs disease data are loading and unstacked

number to separate out some patients from the others. Also, in section Label, we can label the patient's gender and age as it is shown in Figure 2. In the process of mapping our dimensions, we can also map different dimensions that could be a group, X-axis, Y-axis, and radius of the dataset, more precisely.

4.2 Circle packing

At the start of the work, the dataset is going to be unstacked, and the first type of graph will be generating; the name of this type of graph is called Circle Packing. To compare the values and to represent hierarchies, we used nested circles. This circle packing is used to show the proportion of elements through their position and their areas in a hierarchical structure. Two large circles represent genders in the dataset; and size of the smaller circles represents the age. The bigger circles represent those patients whose age is higher than the rest of the patients. The parameters for this result are shown in Figure 3 as

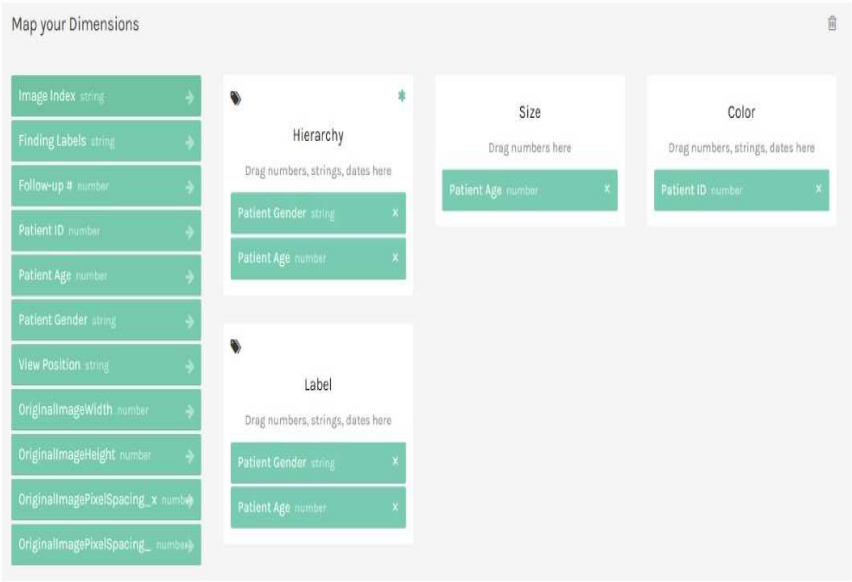

Figure 2. Representation of the dimensions used in RawGraphs

follows.

In this type of graphic representation, the rows that we use for disease from dataset are 3501–5000. To compare the values and to represent hierarchies, we used nested circles to show the proportion of elements through their position and their areas in a hierarchical structure. The graph represents classification of diseases between males and females along with their age groups. As it can be visualized, the disease represented in red circles is most common among males and females, both shown in Figure 4.

4.3 Bee swarm plot

It distributes the elements horizontally, avoiding overlap between them and according to a selected dimension. The x-axis has the age of the patients, and the y-axis has gender. Here, it can be visualized that, in the early ages, the female is supposed to be less likely to be affected by the lung disease as compared to males as shown in Figure 5.

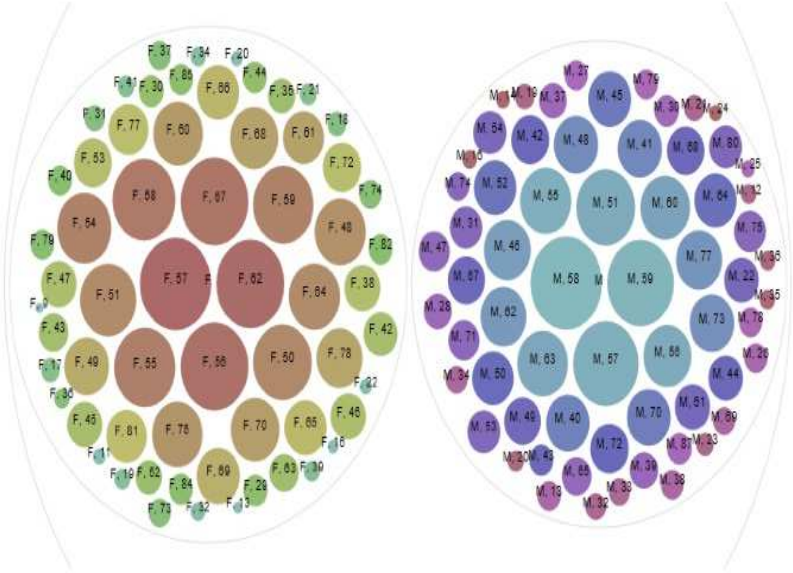

Figure 3. Representation of circle packing Graphs

4.4 Convex hull

In this type of graphic representation, the rows that we use for disease from dataset are 501–1500. In mathematics, the convex hull is the smallest convex shape containing a set of points. It is useful to identify points belonging to the same category when applied to a scatterplot. The shapes represent the same category of disease between females and males of different ages. The x-axis has a patient id, and the y-axis has patient age, as shown in Figure 6. Also, the rows that we use for disease from dataset are 1501–2500; they show the horizontal strokes that represent males and females who have lung disease of the same category, as shown in Figure 7.

4.5 Boxplot

In this type of graphic representation, the rows that we use for disease from dataset are 2501–3000. To summarize a quantitative distribution,

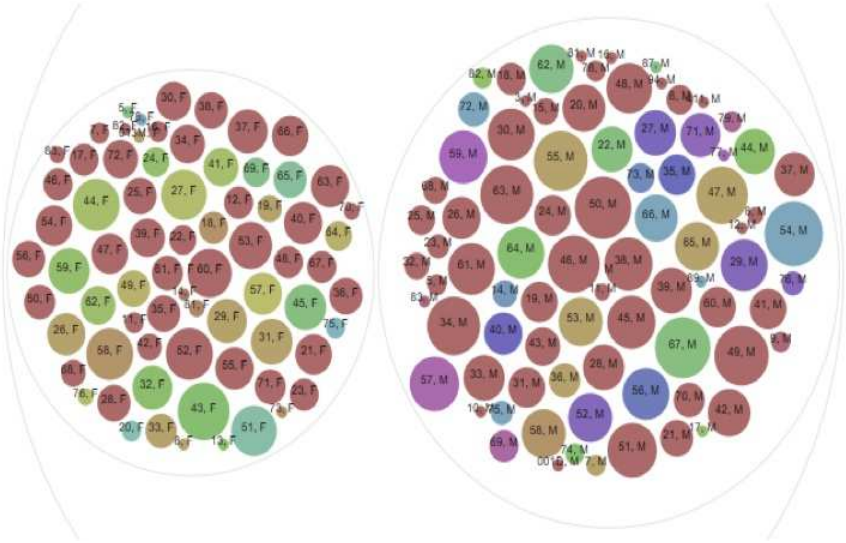

Figure 4. Representation of circle packing Graphs

.

we use five official statistics: the most significant value, upper quartile, median, lower quartile, and the smallest value. Different color of bars represents different diseases, and size of the bar represents age of patients; along the y-axis there is the age and along the x-axis there are the findings of diseases as it is shown in Figure 8.

4.6 Circular dendrogram

In this type of graphic representation, the rows that we use for disease from dataset are 5001–5607. We use this to represent the distribution of hierarchical clustering; the tree-like diagrams use Dendrograms. On the x-axis, the different depth levels represented by each node are visualized. The graph represents the classification of diseases between males and females among the selected data set. The nodes contain names of the diseases which are comprised of males and females, respectively, as it is shown in Figure 9.

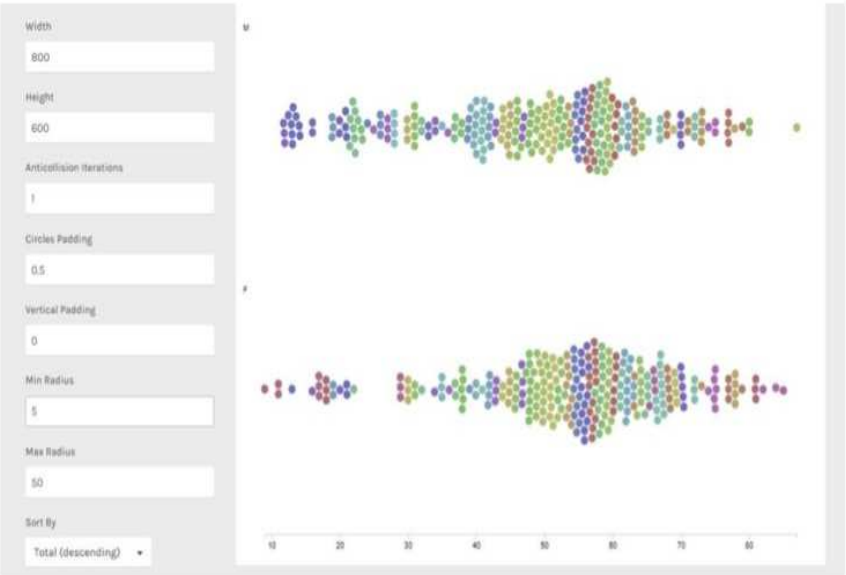

Figure 5. Representation of Bee swarm Plot graphs

5 Conclusion and Future Work

In this paper, we offered RAWGraphs – an Internet program known for its quick production of visualizations out of a data set. The application form is still opensource and can be assumed to become expendable; through, programming skills are also required. We use diverse methods for visualization, which can be circle packing, bee swarm plot, convex hull, boxplot, and circular dendrogram.

Even though end-users' responses are been mostly favorable, by the comments and opinions. We identify about three enhancements to improve long-term function. To begin with, inside today's edition, the legends (e.g., coloration mapping) are observable just at the modifying surroundings; they are lost when the graph has been already exported. Additionally, tags are obvious things that are difficult to take care of, and also new purposes should be supplied to ease tackling, pruning, and

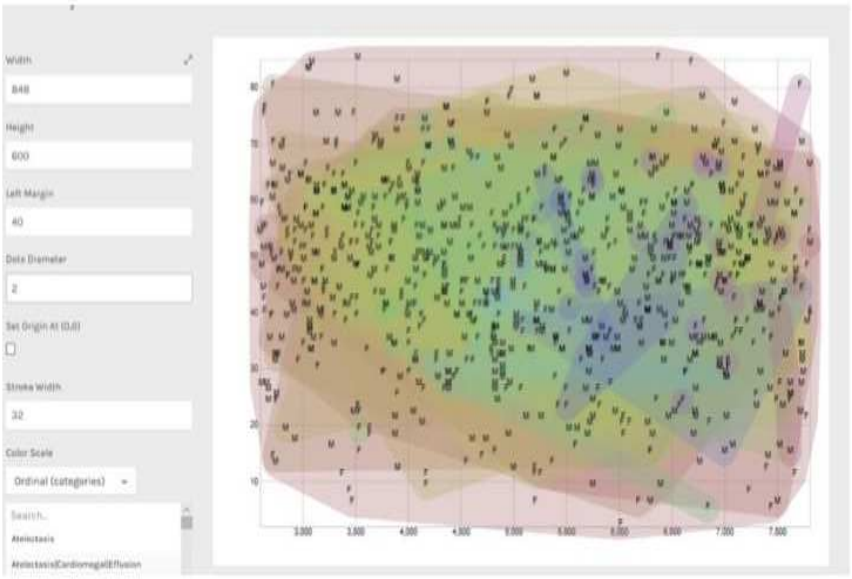

Figure 6. The same category of disease between males and females

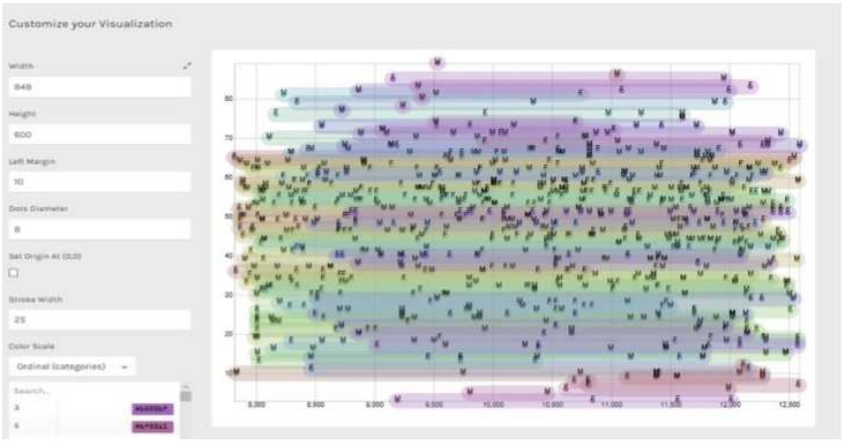

Figure 7. The horizontal strokes represent males and females who have the same category of disease

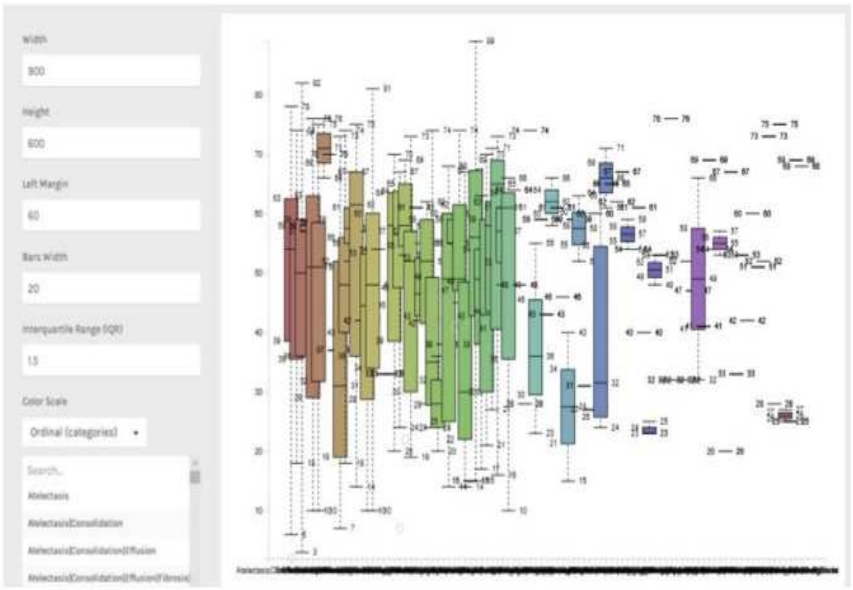

Figure 8. Different color of bars represents different diseases, and size of the bar represents age of patients

filtering. Until now, quite a few subscribers have established their very own customized edition of the application, plus they have added new visual variations; nonetheless, it is still hard for noninvasive end users to authenticate those bits of code. The commencement of advanced visualizations can add a competitive advantage in new graphs. However, it seems to be a beneficial advancement. At length, probably, the engaging obstacle would be to expand the present procedure. Therefore, users may cause interactive visualizations, perhaps not static websites. That necessitates incorporating the capacity to export a package comprising all of the data files (HTML and JavaScript) together with all the mapping. That will allow end-users to manually map measurements, maybe not solely on visible options but in addition to connections (for example, tool-tips or behaviors within an assortment). The comprehension about programming languages is desired; nonetheless,

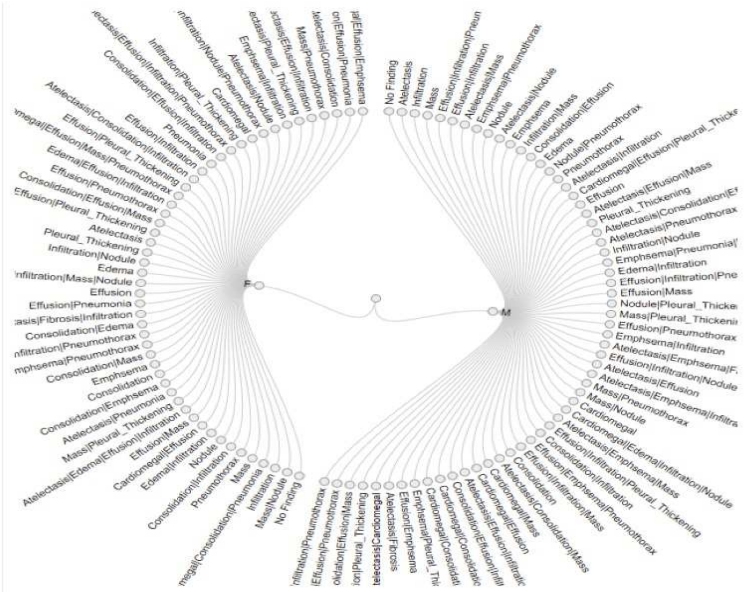

Figure 9. Represents the classification of diseases between males and females

nevertheless, it would be scalable based on the amount of data users wish to alter. The logical approaches adapting by those people already implemented from the present phase of the job could be further researched together to launch new methods for a far more technical direction of developing a design and style, especially inside the discipline of information visualization.

References

[1] M. Mauri, T. Elli, G. Caviglia, G. Uboldi, and M. Azzi, "Rawgraphs: A visualisation platform to create open outputs," in *ACM International Conference Proceeding Series*, ACM, Ed. ACM, September 2017, pp. 1–5. DOI: 10.1145/3125571.3125585.

[2] G. Halkos, S. Managi, and K. Tsilika, "Spatiotemporal distribution of inclusive wealth data: An illustrated guide," MPRA Paper, 2018. [Online]. Available: https://mpra.ub.uni-muenchen.de/85711/1/MPRA_paper_85711.pdf. Accessed on: July 2020.

[3] A.-Y. Guo, Q.-H. Zhu, X. Chen and J.-C. Luo, "Gsds: a gene structure display server," *Yi chuan*, vol. 29, no. 8, p. 1023–1026, 2007. DOI: 10.1360/yc-007-1023.

[4] H. J. Dananberg and M. Guiliano, "Chronic low-back pain and its response to custom-made foot orthoses," *J. Am. Podiatr. Med. Assoc.*, vol. 89, no. 3, pp. 109–117, 1999. DOI: 10.7547/87507315-89-3-109.

[5] H. P. Klug and L. E. Alexander, *X-Ray Diffraction Procedures: For Polycrystalline and Amorphous Materials*, 2nd ed., Wiley, 1974, 992 p. ISBN-13: 978-0471493693. ISBN-10: 0471493694

[6] M. Schlumberger, O. Arcangioli, J. D. Piekarski, M. Tubiana, and C. Parmentier, "Detection and treatment of lung metastases of differentiated thyroid carcinoma in patients with normal chest x-rays," *J. Nucl. Med.*, vol. 29, no. 11, pp. 1790–1794, 1988.

[7] C. Archer, A. R. Levy, and M. McGregor, "Value of routine preoperative chest x-rays: a meta-analysis," *Can. J. Anaesth.*, vol. 40, no. 11, pp. 1022–1027, 1993. DOI: 10.1007/BF03009471.

[8] D. S. Strain, G. T. Kinasewitz, L. E. Vereen, and R. B. George, "Value of routine preoperative chest x-rays: a meta-analysis," *Crit. Care Med.*, vol. 13, no. 7, pp. 534–536, 1985. DOI: 10.1097/00003246-198507000-00004.

[9] K. Mori, J. Hasegawa, J. Toriwaki, H. Anno, and K. Katada, "Automated extraction and visualization of bronchus from 3d ct images of lung," in *International Conference on Computer Vision, Virtual Reality and Robotics in Medicine*, 1995, pp. 542–548. DOI: 10.1007/978-3-540-49197-2_71.

[10] L. Salvolini, E. Bichi Secchi, L. Costarelli, and M. De Nicola, "Clinical applications of 2d and 3d ct imaging of the airways – a review," *Eur. J. Radiol.*, vol. 34, no. 1, pp. 9–25, 2000. DOI: 10.1016/S0720-048X(00)00155-8.

[11] C. T. Badea, M. Drangova, D. W. Holdsworth, and G. A. Johnson, "In vivo small-animal imaging using micro-ct and digital subtraction angiography," *Phys. Med. Biol*, vol. 53, no. 19, pp. 319–350, 2008. DOI: 10.1088/0031-9155/53/19/R01.

[12] D. W. Holdsworth and M. M. Thornton, "Micro-ct in small animal and specimen imaging," *Phys. Med. Biol*, vol. 20, no. 8, pp. 34–39, 2002. DOI: 10.1016/S0167-7799(02)02004-8.

[13] R. A Robb, E. A. Hoffman, L. J Sinak, L. D Harris, and E. L Ritman, "High-speed three-dimensional x-ray computed tomography: The dynamic spatial reconstructor," in *Proc. IEEE*, vol. 71, no. 3, pp. 308–319, 1983. DOI: 10.1109/PROC.1983.12589.

[14] A. Poglitsch et al., "The photodetector array camera and spectrometer (pacs) on the herschel space observatory," *Astron. Astrophys.*, vol. 518, no. 4, pp. 1–12, 2010. DOI: 10.1051/0004-6361/201014535.

[15] G. G. Chowdhury, "Strathprints institutional repository natural language processing," *Annual Review of Information Science and Technology, John Wiley and Sons, Ltd*, vol. 37, no. 1, pp. 51–89, 2003.

Haneen Hassan Al-Ahmadi,

Department of Software Engineering,
College of Computer Science and Engineering, University of Jeddah
E–mail: hhalahamade@uj.edu.sa

Received November 11, 2019
Accepted March 10, 2020